# Study on Multi-steps Dynamic Compression Deformation Behavior of Ti-5.5Al Alloy

IOP Conf. Series: Materials Science and Engineering **585** (2019) 012017 doi:10.1088/1757-899X/585/1/012017

# Study on Multi-steps Dynamic Compression Deformation Behavior of Ti-5.5Al Alloy

**Yumeng Luo**[a, *]

[a]State Key Laboratory for Fabrication and Processing of Nonferrous Metals, GRIMAT Engineering Co., Ltd, Beijing, China
*Email: 672789233@qq.com

**Abstract**. The microstructure evolution in a specific area with typical characteristics of the Ti-5.5Al alloy was studied under multi-steps dynamic compression condition at a strain rate of 4000$s^{-1}$ by EBSD/SEM method. Both twinning and dislocation movement were proved to be the deformation mechanism. However, the dominant deformation mechanism was greatly influenced by strain. During the strain level from 0 to 0.05, the most important deformation mechanism of Ti-5.5Al alloy was dislocation slip. During the deformation process of strain 0.05 to 0.10, the main deformation mechanisms were the $\{10\bar{1}2\}$ of twin and dislocation movement. The rapid expansion of existing twins causes significant changes of texture. During a strain level from 0.10 to 0.15, the main deformation mechanism was twinning, while the dislocation movement dominated the deformation when the strain increased from 0.15 to 0.20. Besides, dislocation was proved to active prior to twinning.

## 1. Introduction

Owing to the high strength and low density, Titanium and its alloy have become indispensable structural materials in many important engineering objects such as space rocket, aircraft and military ground vehicles using under a high strain rate condition. In order to predict the reliability in such services, it is significantly necessary to make a detailed study of dynamic deformation behavior of titanium. The dynamic deformation process contains not only the dynamic mechanical properties but also the deformation mechanism and details of microstructure evolution. However, since the duration of dynamic deformation process of material is very short (often less than 100μs), it is hard for electronic microscope equipment to record the microstructure evolution process. Besides, the loading device in the electronic microscope equipment is difficult to make a sample deformed at a strain rate higher than 1$s^{-1}$. Thus, there is not an effective method to investigate the microstructure evolution during a dynamic deformation process, while an In-Situ [1-5] method can be used to describe the evolution of microstructure (including the nucleation and expanding of twin, the movement of dislocation, and the reaction of twin and dislocation) under quasi-static condition thoroughly.

Meanwhile, several studies focused on the dynamic deformation behavior of Ti alloy have been conducted, and similar conclusions are given [6-8]. First, the twinning system becomes prevalent at high strain rate in crystalline solids. Second, four types of deformation twins have been observed in the dynamic deformed Ti sample, including $\{10\bar{1}2\}$, $\{11\bar{2}1\}$, $\{11\bar{2}2\}$ and $\{11\bar{2}4\}$. Besides, N. P. Gurao [6] studied the change of microstructure and texture during room temperature compression of commercially pure Ti under both quasi-static and dynamic loading conditions, and found that there was a significant difference in the strength of the texture for different orientations which was absent for low strain rate deformed samples at high strain rate. Zhou [7] studied the twin interactions in pure Ti under high strain rate compression, and results show that twinning variants that do not follow the

Schmid law are more frequently observed under high strain rate deformation than quasi-static deformation. However, according to the work listed above, the microstructure evolution under dynamic condition is still not clear, and the dynamic deformation behavior cannot be revealed comprehensively. Thus, in this study, dynamic multi-stepped compression was conducted on a Ti-5.5Al alloy, which is a α-Ti alloy, to a strain of 0.20, and the microstructures at each deformation level were carefully recorded. In this way, the microstructure evolution process was analyzed.

## 2. Experimental Procedure

Since there is still not a suitable method to investigate the dynamic deformation behavior of material, in order to observe and analyze the evolution of microstructure during the dynamic deformation process, a dynamic multi-stepped compression was conducted in this study. A same selected area with typical characteristics of the sample was observed by SEM/EBSD method before and after each step of deformation. Though the microstructure evolution of multi-stepped deformation process is not exactly same to that of the once-wheel deformation, it also can help us to make some new understanding of dynamic deformation behavior.

### *2.1 Material*

The material investigated in this work is Ti-5.5Al alloy supplied as a plate in hot-rolled condition. The components of the alloy are shown in Table 1. Since the transition point of the alloy is measured to be 1010°C, an annealing treatment was applied at 980°C/1h after rolling. The microstructure of the annealed material is shown in Figure 1, which is comprised of equiaxed single-phase α-Ti with an average grain size of about 65 um.

**Table 1.** The components of Ti-5.5Al alloy (wt %)

| Al | C | H | N | O | Ti |
|---|---|---|---|---|---|
| 5.54 | 0.0110 | <0.001 | <0.003 | 0.024 | Bal. |

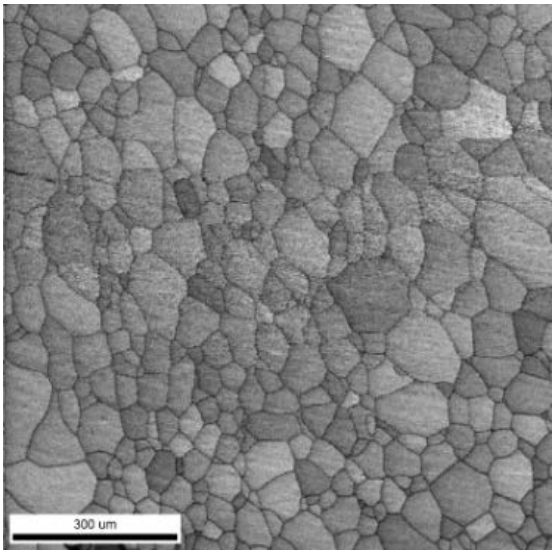


**Figure 1.** Microstructure of the sample used in this study

### *2.2 Specimen*

The layout of the specimen used in this investigation is shown in Figure 2. The surface with a dimension of 3mm*5mm was the observation surface (named Surface A), and was prepared by SiC paper grinding following with electrolytic polishing (volume ratio of perchloric acid: acetic acid equals to 5:95, at 65 V) for SEM and EBSD measurement. Then, a diamond cone indenter was used to make a little mark (width about 20μm) on Surface A. Near this mark, a 1mm*1mm area was selected

as the observation area (named Area B). It must be pointed out that the distance from each boundary of the surface to Area B is not less than 0.5mm.

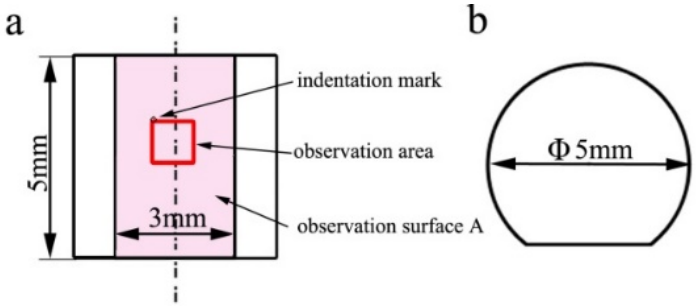


**Figure 2.** Main view (a) and vertical view (b) of the specimen

*2.3 Dynamic Multi-stepped Compression*

In this research, high strain rate compression was conducted along the axial direction of the specimen at room temperature, utilizing a SHPB (Split Hopkinson Pressure Bar). Figure 3a shows the schematic diagram of the SHPB device. The strain rate of every dynamic loading was $4000s^{-1}$, ensured by setting the same impacting velocity. In order to control the axial deformation and also the strain, several strain stopper rings made of maraging steel was placed on the outer circumference of the specimen, as shown in Figure 3b. The height of these strain stopper rings were 4.75mm, 4.50mm, 4.25mm and 4.00mm, respectively, to ensure the whole strain of 0.05, 0.10, 0.15 and 0.20. The inner diameter of these strain stopper rings were all 8mm, to ensure a free radial deformation of the specimen. The contact surface between the strain stopper ring and bars was lubricated by Vaseline. After a step of dynamic loading process, the specimen should be cleaned with Acetone but without electrolytic polishing again.

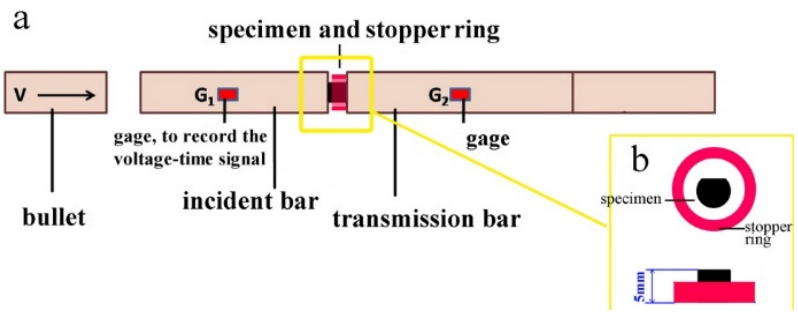


**Figure 3.** Schematic diagram of the SHPB device (a) and stopper ring (b)

*2.4 Microstructure Observation*

SEM equipment used in this investigation was JSM-6510, while EBSD scans were performed with scan step size 2 um in a JSM-7001F field emission scanning electron microscopy equipped with an EDAX/TEAM data acquisition system. The orientation data were analyzed using EDAX/TSL OIM Analysis 6.2 software.

To obtain the original microstructure information, EBSD scan was performed at Area B before compression. Then, after each step of deformation, SEM was used to observe and record the slip lines in Area B in order to investigate the dislocation movement, while EBSD was used to analyze the crystal orientation information.

In order to investigate the dynamic deformation behavior, it is important to identify the slip system and twinning variants. The slip system was determined by the vector of slip lines since this vector must be parallel to the slip plane. The twinning variant was determined according to the rules that the parent grain shares the twinning plane with the twin, and the positions of twinning plane in parent grain and active twinning variant must be overlapped on polar figure.

## 3. Results and Discussion

The EBSD IPF maps of a specific area with typical characteristics observed in Area B corresponding to the strain of 0, 0.05, 0.10, 0.15 and 0.20 are shown in Figure 4a-e, respectively. For the convenience of subsequent descriptions, grains in Area B are numbered from 1 to 46 and marked in IPF maps, respectively.

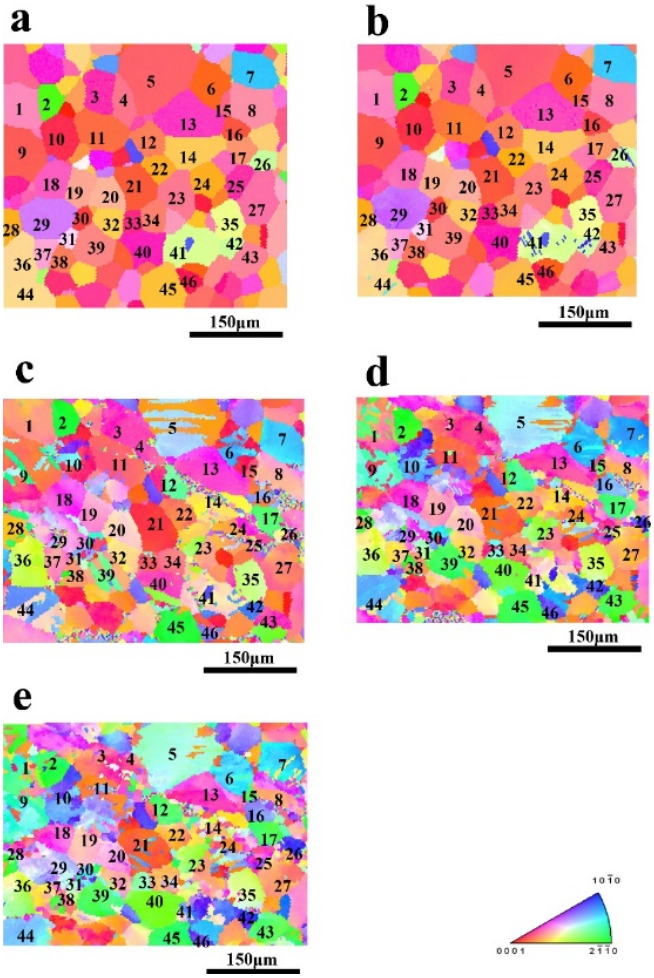


**Figure 4.** IPF images of the multi-stepped deformation specimen with a strain of (a): 0, (b): 0.05, (c): 0.10, (d): 0.15 and (e): 0.20

Combined with SEM results, EBSD data are used to analyze the dynamic deformation behavior. The deformation process from a strain of 0 to 0.05 can be analyzed according to Figure 4a and 4b. Most of the grains show uniform colors. According to the crystal orientation data, the average angle of rotation is about 1° from the beginning to a strain of 0.05. Besides, several twins can be observed in the IPF map with a strain of 0.05, and the twinning systems of each twin are identified by EDAX/TSL OIM Analysis 6.2 software. For easily analyzing, the 6 grains containing $\{10\bar{1}2\}$ twins are painted green in Figure 5. Thus, twinning actives in only 13% of grains, which accounted for 15% of the total area, indicating twinning is not a dominant deformation mechanism at a deformation strain level from 0 to 0.05. According to SEM results, slip lines are found in large amount of grains, as shown in Figure 6. Moreover, in most of grains, the slip lines have only one orientation, indicating that at this deformation level, only one slip system actives in most of the grains. According to the orientation of slip lines, over 60% of slip lines are identified to belong to a pyramidal slip system. The large number of slip lines indicates that, at the deformation strain level from 0 to 0.05, dislocation slip is an important deformation mechanism. However, the interaction between twinning and dislocation slip has not been observed.

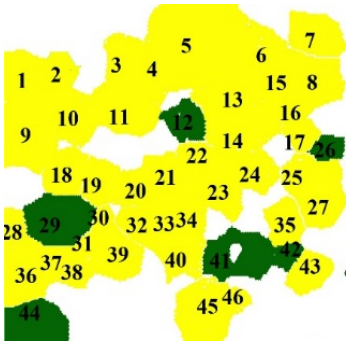


**Figure 5.** Grains with twins. The places painted green indicating the grains contain {10-12} twins and is without twins, respectively

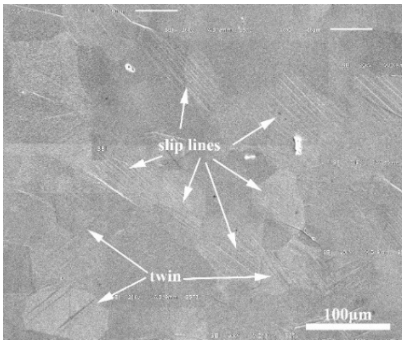


**Figure 6.** Microstructure of the 0.05 strain sample with twins and slip lines

When the strain increases from 0.05 to 0.10, as shown in Figure 4b-c, the color of grains in the IPF map is not uniform again, and the average rotation angle of the matrix is 7.44°. Meanwhile, new $\{10\bar{1}2\}$ twins nucleates in Grain No. $5^{\#}$, $6^{\#}$, $9^{\#}$, $10^{\#}$, $16^{\#}$, $17^{\#}$, $23^{\#}$, $24^{\#}$, $28^{\#}$, $30^{\#}$, $33^{\#}$, $38^{\#}$, $39^{\#}$, $40^{\#}$, $43^{\#}$, $45^{\#}$ and $46^{\#}$. Till a strain of 0.10, 50% of grains are with twins, and all the twins belong to $\{10\bar{1}2\}$ twinning system. However, secondary twinning has not been observed at this strain level, while secondary twinning is very common in pure Ti with a stain of 0.10. Then, SEM figure which was captured at a deformation strain of 0.10, as shown in Figure 7, is used to analyze the dislocation slip behavior combined with grain orientation data determined by EBSD method. It is obvious that, a large amount of new slip lines form at a deformation stage from a strain of 0.05 to 0.10, and over half of the slip lines indicating a pyramidal slip system. Moreover, the steps of slip lines become more obvious, indicating a violent dislocation movement. Thus, twinning and dislocation are both the main deformation mechanism at a strain stage from 0.05 to 0.10. Besides, the interaction of dislocation slip and twinning behavior can be observed at this deformation stage. Figure 8 shows the twins and slip lines at a same place with a strain of 0.05 and 0.10. Twins can be observed at the place where slip lines have already formed at a strain of 0.05. This phenomenon indicates that the slip lines formed earlier than the twins.

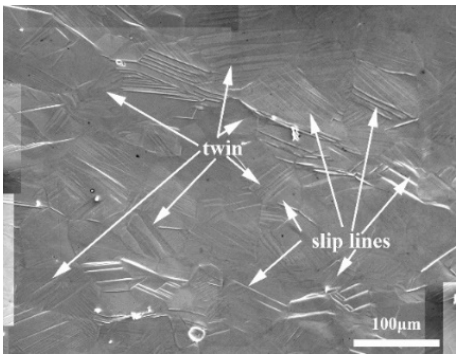


**Figure 7.** Microstructure of the 0.10 strain sample with twins and slip lines

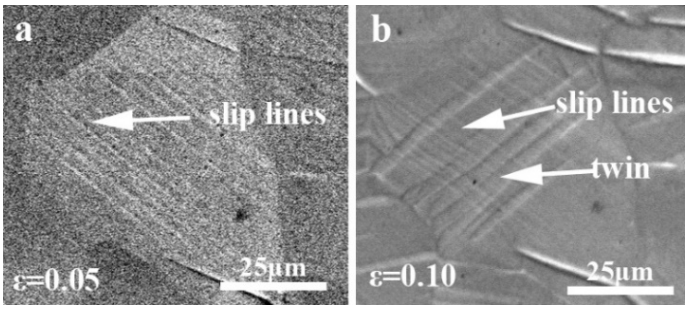


**Figure 8.** The relationship between twinning and dislocation SEM with a strain of (a) 0.05 and (b) 0.10

When the strain increases from 0.10 to 0.15, as shown in Figure 4c-d, the color of IPFs changes greatly, indicating a drastic change in texture. According to the orientation data, the rotation angle is about 67°, but the average rotation angle of the matrix is only 5.7°. By analyzing the twinning behavior in this deformation stage, it can be found that 5 new twins nucleate. So far, there are 28 grains contain twins, accounting for 61% of the total. Moreover, in 13 grains, the existing twins have grown up to nearly occupy the whole matrix, and more than half of the grains have twin areas accounting for more than 50% of the total area. The above phenomena show that twinning is the main deformation mechanism in this deformation stage, and the rapid growth of existing twins is the important reasons for the remarkable change in texture. Figure 9 shows the SEM image of the specimen with a strain of 0.15. Contrast with Figure 7, it is obvious that the morphology of the surface does not change significantly. Only the expansion of the existing twins and the increase of the slip step height can be observed, which indicates that little new dislocation source active in this deformation stage. Thus, compared with the twin behavior, the dislocation movement in this stage is not significant.

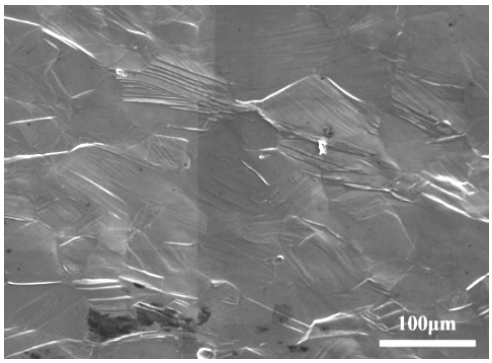


**Figure 9.** SEM image of the observation area, corresponding to a strain of 0.15

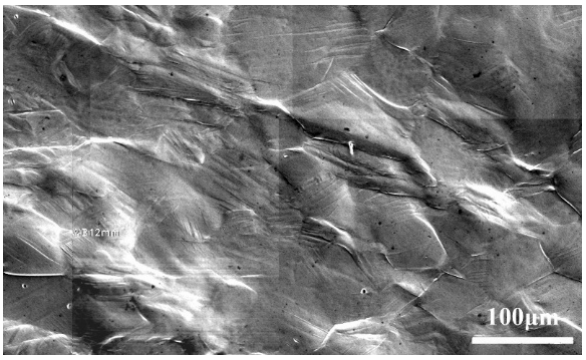


**Figure 10.** SEM image of the observation area, corresponding to a strain of 0.20

When the strain increases from 0.15 to 0.20, as shown in Figure 4d-e, the macro-orientation of the samples does not change significantly at this stage. Since a large number of twins have grown sufficiently in the previous stage, the growth of twins is not obvious in the stage of strain increasing from 0.15 to 0.20. Moreover, the nucleation process of new twins are no longer significant, only a new $\{11\bar{2}1\}$ twin have been observed. The above phenomena show that although twinning still contributes to the deformation in this stage, it is no longer significant compared with the deformation process of strain 0.10 to 0.15.

The dislocation behavior of strain 0.15 to 0.20 is analyzed according to SEM images, as shown in Figure 10. Compared with Figure 9, when the strain increases from 0.15 to 0.20, the surface roughness becomes more serious and the slip step becomes more obvious. A large amount of grains contains slip

lines in two or more orientation, indicating that a large number of new dislocation systems active at this stage. Therefore, the contribution of dislocation motion to deformation is more significant than that of twinning.

According to the above analysis, the multi-stepped dynamic deformation process diagram of Ti-5.5Al alloy is given in Figure 11. It can be seen from the figure that strain has a significant effect on the dynamic deformation mechanism of the alloy: dislocation movement is the main deformation mechanism during the process of strain increasing from 0 to 0.05, but the interaction between dislocation and twinning is not observed. When strain increases from 0.05 to 0.10, the twinning motions, including twinning growth, twinning nucleation are the main deformation mechanism in this stage, and it is evidence that the dislocation motion precedes the twinning. When the strain increases from 0.10 to 0.15, the rapid expansion of existing twins causes significant changes of texture. Twinning is the main deformation mechanism in this stage. Compared with the previous stage, the dislocation motion is not significant when the strain increases from 0.10 to 0.15. When the deformation strain is greater than 0.15, the dislocation becomes the main deformation mechanism.

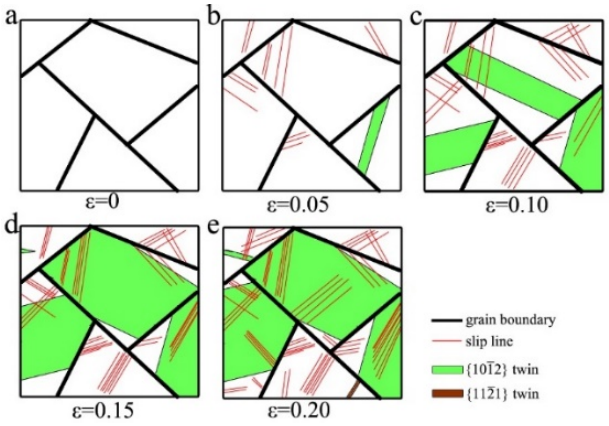


**Figure 11.** Schematic of the dynamic multi-stepped deformation process of Ti-5.5Al alloy

## 4. Conclusion

This paper studies the dynamic multi-stepped compression behavior of Ti-5.5Al alloy. The microstructures at each deformation strain are recorded to reveal the evolution of microstructure under dynamic deformation condition. Results show that twinning and dislocation slip are both the dynamic deformation mechanisms of Ti-5.5Al alloy. However, the main deformation mechanism is greatly influenced by deformation strain. When the strain increases from 0 to 0.05, dislocation movement is the main deformation mechanism. When the strain increases from 0.05 to 0.10, the $\{10\bar{1}2\}$ twinning motions, including twinning growth, twinning nucleation are the main deformation mechanisms in this stage. When the strain increases from 0.10 to 0.15, twinning is the main deformation mechanism in this stage, and the rapid expansion of existing twins causes significant changes of texture. When the deformation strain is greater than 0.15, the dislocation becomes the main deformation mechanism. Moreover, when the Ti-5.5Al alloy is conducted by a dynamic compression loading, it is evidence that the dislocation motion precedes the twinning motion.

## 5. Acknowledgment

The author appreciate the financial support from National Key R&D Program of China (2017YFB0306201), and the National Nature Science Foundation of China (NSFC No. 51601016)

## 6. Reference

[1] Wang S, Zhang Y, Schuman C, et al., Acta Materialia. 82 (2015) 424-436.
[2] Wang L, Lind J, Phukan H, et al., Scripta Materialia. 92 (2014) 35-38.
[3] Meng Y, Gong G, Wei D, et al. Applied Clay Science. 132-133 (2016) 760-767.
[4] Malyar N V, Dehm G, Kirchlechner C, Scripta Materialia. 138 (2017) 88-91.

[5] Zhang K, Ni L, Lei Z, et al., Materials Characterization. 123 (2017) 51-57.
[6] Gurao N P, Kapoor R, Suwas S., Acta Materialia. 59 (2011) 3431-3446.
[7] Zhou P, Xiao D, Jiang C, et al., Metallurgical & Materials Transactions A. 48(2016)1-13.
[8] Xu F, Zhang X, Ni H, et al., Materials Science & Engineering A. 541(2012)190-195.